

## Green Synthesis of Ag Thin Films on Glass Substrates and Their Application in Surface-Enhanced Raman Scattering

Young Kwan Cho, In Hyun Kim, and Kuan Soo Shin\*

Department of Chemistry, Soongsil University, Seoul 156-743, Korea. \*E-mail: kshin@ssu.ac.kr  
Received June 17, 2013, Accepted July 9, 2013

Nanostructured Ag thin films could be facilely prepared by soaking glass substrates in ethanolic solutions containing Ag<sub>2</sub>O powders at an elevated temperature. The formation of zero-valent Ag was corroborated using X-ray diffraction and X-ray photoelectron spectroscopy. The deposition of Ag onto a glass substrate was readily controlled simply by changing the reaction time. Due to the aggregated structures of Ag, the surface-enhanced Raman scattering spectra of benzenethiol could be clearly identified using the Ag-coated glass. The enhancement factor at 514.5 nm excitation estimated using benzenethiol reached  $1.0 \times 10^5$  while the detection limit of rhodamine 6G was found to be as low as  $1.0 \times 10^{-13}$  M. Since this one-pot fabrication method is eco-friendly and is suitable for the mass production of diverse Ag films, it is expected to play a significant role in the development of surface plasmon-based analytical devices.

**Key Words** : Ag thin film, Ag<sub>2</sub>O powder, Ethanol, Surface-enhanced Raman scattering

### Introduction

Noble metallic nanostructures exhibit a phenomenon known as surface-enhanced Raman scattering (SERS)<sup>1-3</sup> in which the Raman scattering cross-sections are dramatically enhanced for the molecules adsorbed onto them. In recent years, it has been reported that even single molecule detection is possible by surface-enhanced resonance Raman scattering (SERRS);<sup>4-6</sup> the Raman cross sections are then comparable to the usual cross sections of fluorescence. To use SERS/SERRS in routine, on-line studies for analytical purposes, the substrates should be stable, reproducibly prepared, inexpensive, and easy to make.<sup>7,8</sup> In reality, the enhancement properties of a SERS-active surface are highly correlated to its method of preparation and therefore its detailed nanostructure. Most SERS active surfaces currently available are lacking in stability and/or reproducibility. Electrochemically roughened electrodes usually exhibit high SERS activity, but it is difficult to control the quality of the electrode surfaces.<sup>9,10</sup> Vacuum evaporation can be used to form homogeneous metal surfaces with high SERS activity, but this process requires expensive and specialized apparatus.<sup>11,12</sup> The extent of aggregation of colloidal sols is difficult to control, and the sedimentation of aggregated sols onto solid substrates is not reproducible.<sup>13,14</sup>

Although the well-known mirror reaction (Tollens process) and Sn<sup>2+</sup>-mediated electroless plating have been reported to form robust silver films on silicon wafers or glasses,<sup>15</sup> it is not easy to control the surface roughness of the films since more than one-step and complex reagents are needed to accomplish the necessary reactions. Moreover, most silvering baths for electroless plating are highly unstable, so additional protective reagents were needed to minimize the corresponding bulk reductions. Recently, Inoue *et al.*<sup>16</sup> reported that the nanostructured Ag films composed of

nanoparticles and nanorods could be readily formed by the ultrasonication of ethanol solutions containing Ag<sub>2</sub>O particles. They also proposed the reaction mechanisms for the formation of Ag films from Ag<sub>2</sub>O/ethanol slurries using sonoprocess. Park *et al.*<sup>17</sup> also reported that very stable and optically tunable Ag films can be reproducibly fabricated simply by soaking glass substrates in ethanolic solutions of AgNO<sub>3</sub> and butylamine. These Ag films were shown to possess a very homogeneous morphology and SERS activity.

In this paper, we present another very simple and eco-friendly method that can repeatedly produce highly SERS-active Ag films on dielectric substrates such as glass. This method only requires the incubation of negatively charged glass substrates in ethanol solution containing Ag<sub>2</sub>O powders at an elevated temperature. Silver films are then formed exclusively and evenly on glass substrates by the reduction activity of ethanol. Since ethanol is a very mild reductant,<sup>18</sup> bulk reaction does not take place, although the ethanol can reduce silver ions that have been anchored on the negatively charged glass substrates. Due to the aggregated structures of Ag, the as-prepared Ag-coated glass substrates were found to be efficient SERS substrates for the vibrational spectroscopic characterization of molecular adsorbates; in specific, the enhancement factor estimated using benzenethiol (BT) as a model adsorbate reached  $1 \times 10^5$  with a 514.5 nm excitation source. We also demonstrated that Ag-coated glass substrates could be used to detect rhodamine 6G (R6G) molecules, which is often employed in SERS studies, due to its large Raman cross-section, down to concentrations of  $1.0 \times 10^{-13}$  M based on an S/N ratio of 3.

### Experimental

Silver(I) oxide (Ag<sub>2</sub>O, 99%) micrometer-sized powder, BT (98%), and R6G (95%) were purchased from Aldrich

and used as received. Absolute ethanol (99.9%) was purchased from J. T. Baker. Other chemicals, unless specified, were of reagent grade. Highly pure water (Millipore), of resistivity greater than 18.0 M $\Omega$ -cm, was used throughout.

Initially, slide glasses (50 mm  $\times$  10 mm  $\times$  1 mm, Marienfeld) were soaked in a piranha solution for 30 min and sonicated in distilled water for 30 min, followed by rinsing with ethanol, and finally dried in an oven at 60  $^{\circ}$ C for 60 min. The cleaned glasses were dipped in the reaction mixture and incubated for 6 h at 70  $^{\circ}$ C with vigorous shaking. As a reaction mixture, the 23 mg of Ag<sub>2</sub>O powder dispersed in 10 mL absolute ethanol was used for all experiments, but the reaction time was varied, from 15 min to 0.5, 1, 2, 3, or 4 h. Hereafter, the as-prepared Ag-coated glass substrates will be labeled as Ag(15 min), Ag(30 min), Ag(1 h), Ag(2 h), Ag(3 h), and Ag(4 h) films, respectively, according to their reaction time. The Ag-coated glass substrates were finally rinsed with ethanol and air-dried.

For the self-assembly of BT onto Ag-coated glass substrates, they were immersed in 10 mM ethanolic solution of BT for about 30 min and then washed with deionized water several times and dried in air. To examine the detection limit of R6G molecules in water by SERS technique, various concentrations of R6G were prepared; the concentrations were of 10<sup>-7</sup>, 10<sup>-8</sup>, 10<sup>-9</sup>, 10<sup>-10</sup>, 10<sup>-11</sup>, 10<sup>-12</sup>, and 10<sup>-13</sup> M. For each test, the Ag-coated glass substrates were immersed in R6G aqueous solution for 2 h and then dried naturally. Raman spectra were obtained using a Renishaw Raman system 2000 spectrometer equipped with an integral microscope (Olympus BH2-UMA). The 514.5 nm line from a 20 mW Ar<sup>+</sup> laser (Melles-Griot Model 351MA520) was used as the excitation source. The laser beam was focused onto a spot approximately 1  $\mu$ m in diameter. The Raman band of a silicon wafer at 520 cm<sup>-1</sup> was used to calibrate the spectrometer; the accuracy of the spectral measurements was estimated to be better than 1 cm<sup>-1</sup>. Field-emission scanning electron microscopy (FE-SEM) images were measured using a JSM-6330F field-emission scanning electron microscope operating at 2 kV. X-ray diffraction (XRD) patterns were obtained on a Rigaku Model MiniFlex powder diffractometer using Cu K $\alpha$  radiation. X-ray photoelectron spectroscopy (XPS) measurements were carried out with an AXIS-His model using a Mg K $\alpha$  X-ray as the light source. UV-visible (UV-vis) absorption spectra were obtained using an Avantes 3648 spectrometer. Atomic force microscopy (AFM) images were obtained on a Photonitech NANOSTATION II system. Using an 125 mm long etched silicon cantilever with a nominal spring constant of 20-100 N/m (Nanoprobe, Digital Instruments), topographic images were recorded in a tapping mode with a driving frequency of  $\sim$ 300 kHz at a scan rate of 2 Hz.

## Results and Discussion

In this study, an eco-friendly one-pot strategy to produce nanostructured Ag thin film is developed from Ag<sub>2</sub>O powders using ethanol as a reducing agent. Figure 1 shows an

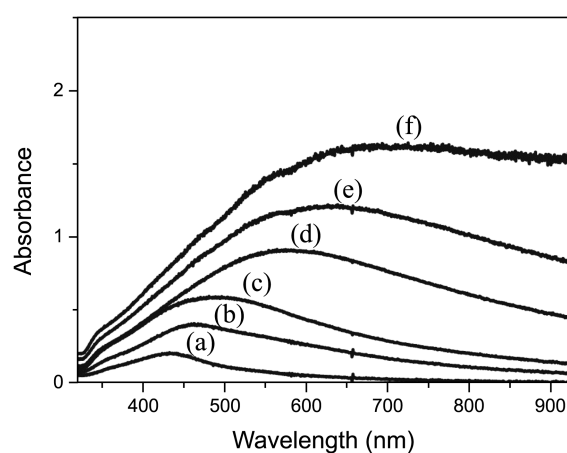


**Figure 1.** Temporal evolution of UV-vis spectra of Ag films with different reaction times; (a) Ag(15 min), (b) Ag(30 min), (c) Ag(1 h), (d) Ag(2 h), (e) Ag(3 h), and (f) Ag(4 h) films deposited on glass substrates.

increase of the absorbance peak intensity with the reaction time. The Ag(15 min) film exhibits an absorption maximum at 436 nm, due to Mie plasmon resonance excitation from the Ag nanoparticles.<sup>19</sup> For Ag(30 min), Ag(1 h), Ag(2 h), Ag(3 h), and Ag(4 h) films, the absorption maximum is red-shifted to 461, 481, 566, 615, and 670 nm, respectively. The position of the maximum peak is gradually red-shifted with an increase of the size of the Ag nanoparticles deposited on glass substrates.<sup>20</sup> In addition, as the Ag nanoparticles coalesce into a network-like structure on the surfaces of glass substrates, a distinct peak is no longer observed. Instead, a broad band appears, extending to near-infrared regions. The different optical properties of the six films can also be discerned by the naked eye; the color of the films varied from yellow to deep blue in accordance with the red shift of the absorption maximum.

Figure 2 shows the typical FE-SEM images of the Ag thin film deposited on glass substrates using Ag<sub>2</sub>O powders and ethanol with various reaction times from 15 min to 4 h. It was observed that the cluster size and the degree of aggregation of Ag nanoparticles largely depend on the reaction time. The mean granular sizes of Ag nanostructures were determined to be 37.9  $\pm$  4.4, 59.4  $\pm$  7.5, 67.8  $\pm$  9.3, 82.3  $\pm$  13, 152  $\pm$  26, and 187  $\pm$  28 nm, suggesting that larger silver nanoclusters are produced by increasing the reaction time. The formation of Ag nanoparticles from Ag<sub>2</sub>O powders using ethanol can be confirmed by the XRD patterns and the XPS spectra of an Ag(4 h) film as shown in Figure 3. The XRD patterns, which is characterized by the four peaks positioned at 38.1 $^{\circ}$ , 44.3 $^{\circ}$ , 64.4 $^{\circ}$ , and 77.4 $^{\circ}$ , in Figure 3(b) can be assigned to the reflections from the (111), (200), (220), and (311) lattice planes, respectively, of the face centered cubic Ag particles (JCPDS file 04-0783).<sup>21</sup> The crystallite size of Ag nanoparticles calculated from the Scherrer equation,<sup>22</sup> using the half width of the intense (111) reflections, was about 20 nm, which was smaller than the apparent cluster sizes of Ag thin films confirmed from FE-SEM images ( $\sim$ 187 nm). This is probably because the cluster

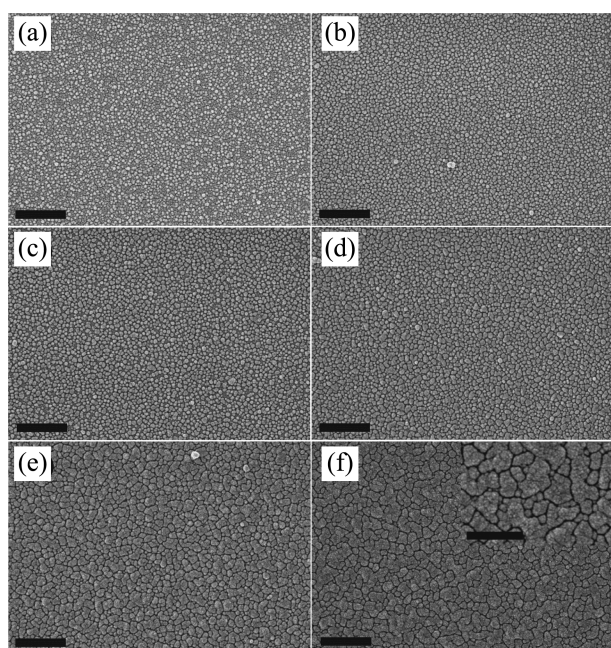


**Figure 2.** FE-SEM images of Ag films with different reaction times; (a) Ag(15 min), (b) Ag(30 min), (c) Ag(1 h), (d) Ag(2 h), (e) Ag(3 h), and (f) Ag(4 h) films deposited on glass substrates; the scale bar = 500 nm. Inset in (f) shows the magnified image of Ag(4 h) film; the scale bar = 100 nm.

forms of Ag films are actually comprised of 20 nm-sized Ag crystallites (See inset of Figure 2(f)). For reference, the XRD patterns of  $\text{Ag}_2\text{O}$  powders purchased from Aldrich are shown in Figure 3(a); all peaks correspond to those reported for bulk  $\text{Ag}_2\text{O}$  with a cubic structure (JCPDS file 12-0793).<sup>23</sup> To further confirm the formation of Ag atoms from  $\text{Ag}_2\text{O}$ , XPS was used to examine the change in oxidation state for Ag after the reduction reaction had occurred.<sup>24</sup> According to XPS measurements, the XPS peaks at 368 and 374 eV in Figure 3(c) can be assigned, respectively, to the Ag  $3d_{5/2}$  and Ag  $3d_{3/2}$  peaks of zero-valent Ag.<sup>24</sup>

Nanostructured Ag thin films on glass substrates are expected to be formed from the reduction of silver ions produced by the slow dissolution of  $\text{Ag}_2\text{O}$  powders in ethanol at an elevated temperature. The hydroxyl groups of the glass surfaces are partially deprotonated in absolute ethanol, leaving behind a lot of negatively charged surface oxygen atoms. Upon adding silver ions, the oxygen sites are bound by silver ions such that the surface-bound silver ions can subsequently function as seeds for the growth of Ag nanostructures on the surface of a glass by the action of a mild reductant, *i.e.* ethanol. It should be mentioned that the reaction mechanism of  $\text{Ag}^+$  ions in ethanol solutions prepared using  $\text{AgNO}_3$  is quite different from that of ethanol solutions containing  $\text{Ag}_2\text{O}$ . As reported by Inoue *et al.*, the  $\text{Ag}^+$  ions in ethanolic solution of  $\text{AgNO}_3$  are difficult to reduce even under the sonication condition.<sup>16</sup> The presence of counter ions, such as  $\text{NO}_3^-$ , is likely to substantially reduce the reactivity between ethanol and  $\text{Ag}^+$  ions in the formation process of Ag nanostructures. Once Ag nanostructures are

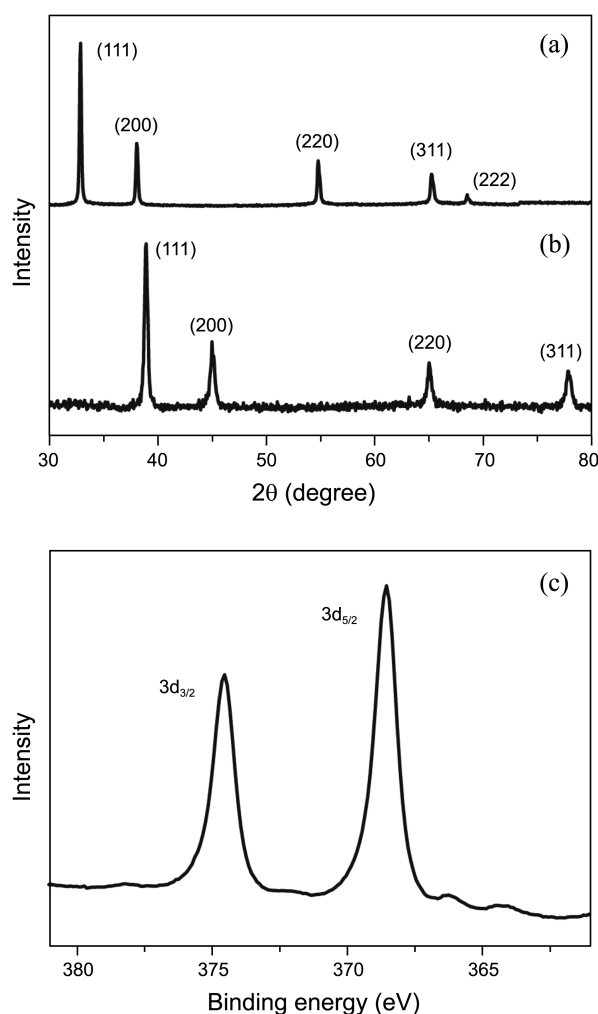


**Figure 3.** XRD patterns of (a)  $\text{Ag}_2\text{O}$  powder and (b) an Ag(4 h) film deposited on a glass substrate. (c) XPS spectrum of an Ag(4 h) film deposited on a glass substrate.

formed, an analyte solution can be introduced onto the silver surface for chemisorption or physisorption of the analyte molecules that can subsequently be detected by SERS.

Considering the fact that SERS usually occurs with aggregated structures of Ag particles in the range of 20–200 nm, the as-prepared Ag-coated glass substrates would be expected to show higher SERS activity. The performance of our silver thin films as SERS substrates was evaluated using BT as a model compound.<sup>17,25</sup> Figure 4(a) shows the typical SERS spectra of BT adsorbed on Ag(15 min), Ag(30 min), Ag(1 h), Ag(2 h), Ag(3 h), and Ag(4 h) films, respectively. The bands at 998, 1021, 1072, and 1573  $\text{cm}^{-1}$  can be assigned to the in-plane ring-breathing mode, the in-plane C–H bending mode, the in-plane ring-breathing mode coupled with the C–S stretching mode, and the C–C stretching mode, respectively.<sup>26</sup> As can be seen in Figure 4(b), the most intense SERS peaks of BT are observed from an Ag(4 h), while the peaks from Ag(15 min) film are extremely weak. These observations indicate that substrate containing larger cluster size and network-like structure exhibits higher surface enhancement. It is also notable that Ag(1 h) film shows

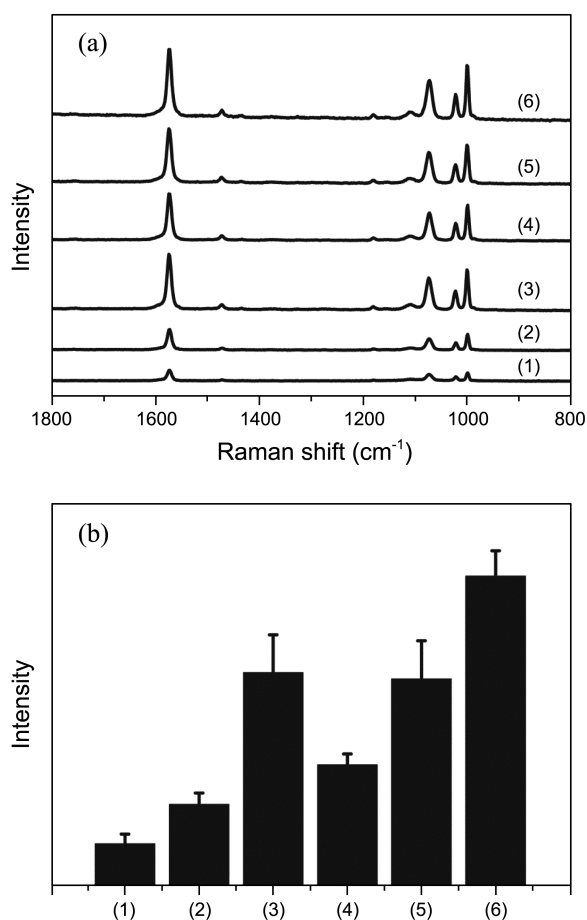


**Figure 4.** (a) SERS spectra of BT adsorbed on (1) Ag(15 min), (2) Ag(30 min), (3) Ag(1 h), (4) Ag(2 h), (5) Ag(3 h), and (6) Ag(4 h) films. (b) Relative Raman peak intensities of benzenethiol at  $1574\text{ cm}^{-1}$  ( $v_{8a}$ ) measured using (1) Ag(15 min), (2) Ag(30 min), (3) Ag(1 h), (4) Ag(2 h), (5) Ag(3 h), and (6) Ag(4 h) films. The error bars indicate the average and standard deviation of 5 different measurements.

relatively higher SERS activity compared to other Ag films. The origin of high SERS activity of Ag(1 h) film is not clear; one possible explanation would be that the maximum surface plasmon absorption of Ag(1 h) film (*i.e.*, 481 nm, see Figure 1) matches well with the excitation source (514.5 nm). This is because when an external electromagnetic field that matches the surface plasmon is applied on the Ag nanoclusters an enormous electric field is generated around it.<sup>27</sup> It is known that the induced dipoles oscillating at Raman frequencies which are still within the surface plasmon resonance line width are enhanced by the metal nanoclusters, giving rise to an enhancement of Raman scattering intensity.<sup>28</sup> In addition, the junction between two large Ag clusters acts as a hot spot for the detection of few molecules.<sup>5</sup> The electromagnetic theory predicts that the enhanced field around each particle coherently interferes. As the distance between the Ag nanoclusters decreases, the coupled plasmon resonance shifts to the red and the enhanced electromagnetic field increases at the junction between nanoclusters. The junction can therefore act as an electromagnetic hot spot.

This electric field enhances the Raman signals from BT and hence the intense SERS peaks are observed.

The SERS enhancement factor (EF) of Ag(4 h) film was estimated via the following relationship:

$$EF = (I_{\text{SERS}}/I_{\text{NR}})(N_{\text{NR}}/N_{\text{SERS}})$$

where  $I_{\text{SERS}}$  and  $I_{\text{NR}}$  are the SERS intensity of BT on Ag(4 h) film and the normal Raman (NR) scattering intensity of BT in bulk, respectively, and  $N_{\text{SERS}}$  and  $N_{\text{NR}}$  are the number of BT molecules illuminated by the laser light to obtain the corresponding SERS and NR spectra, respectively.<sup>17,25,29</sup>  $I_{\text{SERS}}$  and  $I_{\text{NR}}$  were measured at  $1574\text{ cm}^{-1}$ , and  $N_{\text{SERS}}$  and  $N_{\text{NR}}$  were calculated on the basis of the estimated concentration of surface BT species, density of bulk BT, and the sampling areas. The equilibrated surface concentration of BT is assumed to be  $\sim 7.1 \times 10^{-10}\text{ mol/cm}^2$ .<sup>29</sup> Taking the sampling area (ca. 1 mm in diameter) as well as the surface roughness factor ( $\sim 3.03$ ) obtained from the AFM measurement of Ag(4 h) film into account,  $N_{\text{SERS}}$  is calculated to be  $1.6 \times 10^{-17}\text{ mol}$ . When taking the NR spectrum of pure BT, the sampling volume will be the product of the laser spot and the penetration depth ( $\sim 15\text{ nm}$ ) of the focused beam. As the density of BT is  $1.07\text{ g/cm}^3$ ,  $N_{\text{NR}}$  is calculated to be  $1.1 \times 10^{-13}\text{ mol}$ . Since the intensity ratio,  $I_{\text{SERS}}/I_{\text{NR}}$ , is measured to be  $\sim 15$  for Ag(4 h) film at 514.5 nm excitation, EF can then be as large as  $1.0 \times 10^5$ . It should be mentioned that, as quoted in Figure 4(d), five different spots were randomly selected to take the SERS spectra for each Ag substrate; the peak intensities at  $1574\text{ cm}^{-1}$  were also normalized with respect to that of a silicon wafer used in the instrument calibration. The fact that the relative standard deviation was less 9% for all Ag films clearly illustrates the homogenous nature of our Ag films.

Based on these promising results, it is worth examining the detection limit of the present Ag films. In this light, we have taken a series of SERRS spectra at various concentrations of R6G ranging from  $10^{-7}$  to  $10^{-13}\text{ M}$  adsorbed on the Ag(4 h) film (see Figure 5(a)). The peaks at 615, 770, and  $1188\text{ cm}^{-1}$  are due to the C–C–C ring in-plane bending, the C–H out-of-plane bending, and the C–C stretching vibrations, respectively.<sup>5,28</sup> The peaks at 1312, 1362, 1503, 1572, and  $1648\text{ cm}^{-1}$  are associated with the symmetric in-plane stretching vibrations of R6G exhibiting the resonance enhancement effect at 514.5 nm excitation. Figure 5(b) shows the log-log graph of the intensity of the R6G peak at  $\sim 1650\text{ cm}^{-1}$  drawn *versus* the concentration of R6G solution. The solid line is the linear fit to the data. It can be seen that the intensity of SERRS signal varies almost linearly with the concentration of R6G over a large concentration change by 7 orders of magnitude. The deviation from the linear fit at lower concentration is relatively larger and may indicate that some of the molecules experience different Raman enhancement due to local inhomogeneity of the electromagnetic field. Nonetheless, we are able to detect as low as  $1.0 \times 10^{-13}\text{ M}$  of R6G with an S/N ratio of  $3.2 \pm 1.0$ ; the detection limit would then be  $1.0 \times 10^{-13}\text{ M}$  based on an S/N ratio of 3. This clearly suggests that our Ag film synthesized eco-friendly

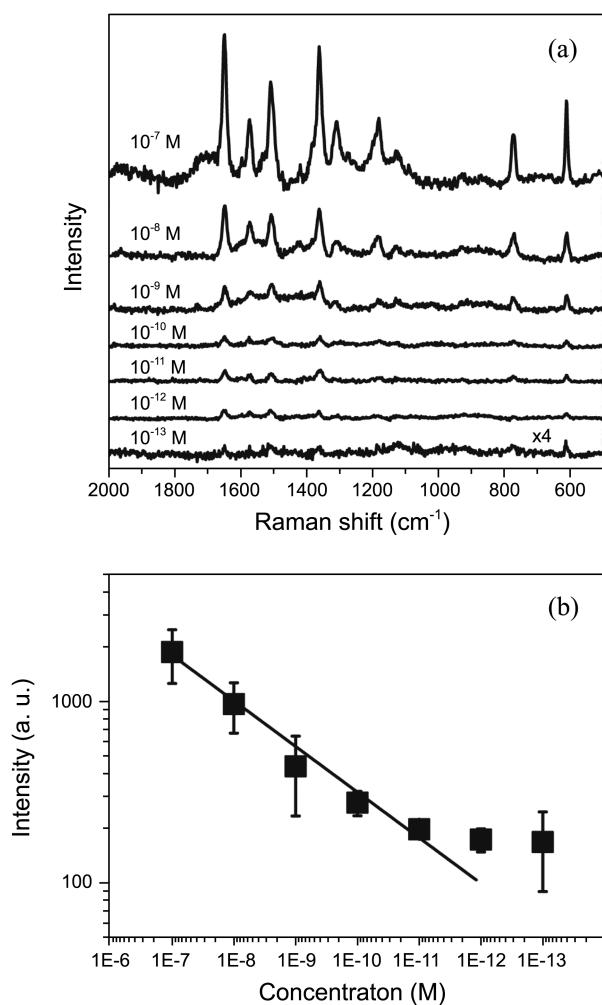


**Figure 5.** (a) Collection of SERRS spectra of R6G at the various concentrations ranging from  $10^{-7}$  to  $10^{-13}$  M adsorbed on the Ag(4 h) film. A 514.5 nm excitation source was used. (b) The intensity of the Raman peak at  $1650\text{ cm}^{-1}$  in (a), normalized with respect to that of a silicon wafer at  $520\text{ cm}^{-1}$ , versus the concentration of R6G. The error bars indicate the average and standard deviation of 3 different measurements.

from  $\text{Ag}_2\text{O}$  powders and ethanol is an invaluable tool for the analysis of effluent chemicals by SERS/SERRS technique.

### Conclusion

In this work, an eco-friendly one-pot strategy to produce nanostructured Ag thin film is developed from  $\text{Ag}_2\text{O}$  powders using ethanol as a reducing agent at an elevated temperature. The deposition of Ag onto the glass substrate was readily controlled simply by changing the reaction time. The formation of zero-valent Ag was confirmed using XRD and XPS analyses. The morphology change of the thin Ag film was monitored using FE-SEM measurements. Due to the aggregated structures of Ag, the SERS spectra of BT could be clearly identified. The enhancement factor estimated using BT reached  $\sim 1.0 \times 10^5$  while the detection limit of

R6G was as low as  $1.0 \times 10^{-13}$  M based on an S/N ratio of 3. The method is eco-friendly and is suitable for the mass production of diverse Ag films. Hence, the method will be useful in the development of plasmon-based analytical devices, specifically SERS-based biosensors.

**Acknowledgments.** This work was supported by National Research Foundation of Korea (NRF) grant funded by the Korea government (MSIP) (No. 2012R1A2A2A01008004).

### References

- Eustis, S.; El-Sayed, M. *Chem. Soc. Rev.* **2006**, *35*, 209.
- Brus, L. *Acc. Chem. Res.* **2008**, *41*, 1742.
- Jiang, J.; Bosnick, K.; Maillard, M.; Brus, L. *J. Phys. Chem. B* **2003**, *107*, 9964.
- Kneipp, K.; Wang, Y.; Kneipp, H.; Perelman, L. T.; Itzkan, I.; Dasari, R. R.; Feld, M. S. *Phys. Rev. Lett.* **1997**, *78*, 1667.
- Michaels, A. M.; Jiang, J.; Brus, L. *J. Phys. Chem. B* **2000**, *104*, 11965.
- Constantino, C. J. L.; Lemma, T.; Antunes, P. A.; Aroca, R. *Anal. Chem.* **2001**, *73*, 3674.
- McNay, G.; Eustace, D.; Smith, W. E.; Faulds, K.; Graham, D. *Appl. Spectrosc.* **2011**, *65*, 825.
- Smith, W. E. *Chem. Soc. Rev.* **2008**, *37*, 955.
- Fleischmann, M.; Hendra, P. J.; McQuillan, A. J. *Chem. Phys. Lett.* **1974**, *26*, 163.
- Norrod, K. L.; Sudnik, L. M.; Rousell, D.; Rowlen, K. L. *Appl. Spectrosc.* **1997**, *51*, 994.
- Stirland, D. J. *Appl. Phys. Lett.* **1966**, *8*, 326.
- Okazaki, H.; Sawada, S.; Kimura, M.; Tanaka, H.; Matsumoto, T.; Ohtake, T.; Inoue, S. *IEEE Electron Device Lett.* **2012**, *33*, 1087.
- Pinkhasova, P.; Yang, L.; Zhang, Y.; Sukhishvili, S.; Du, H. *Langmuir* **2012**, *28*, 2529.
- Stiuftuc, R.; Iacovita, C.; Lucaciu, C.; Stiuftuc, G.; Dutu, A.; Braescu, C.; Leopold, N. *Nanoscale Res. Lett.* **2013**, *8*, 1.
- Mallory, G. O.; Hajdu, J. B., Eds.; *Electroless Plating: Fundamentals and Applications*; American Electroplaters and Surface Finishers Society: Orlando, FL, 1990; Chapter 17.
- Inoue, M.; Hayashi, Y.; Takizawa, H.; Suganuma, K. *Colloid Polym. Sci.* **2010**, *288*, 1061.
- Park, H. K.; Yoon, J. K.; Kim, K. *Langmuir* **2006**, *22*, 1626.
- Wang, S.; Tseng, W. J. *Nanopart. Res.* **2009**, *11*, 947.
- Bohren, C. F.; Huffman, D. R. *Absorption and Scattering of Light by Small Particles*; John Wiley & Sons: Chichester, U.K., 1983.
- Van Duyne, R. P.; Hulst, J. C.; Treichel, D. A. *J. Chem. Phys.* **1993**, *99*, 2101.
- Philip, D.; Unni, C.; Aromal, S. A.; Vidhu, V. K. *Spectrochim. Acta A* **2011**, *78*, 899.
- Borchert, H.; Shevchenko, E. V.; Robert, A.; Mekis, I.; Kornowski, A.; Grübel, G.; Weller, H. *Langmuir* **2005**, *21*, 1931.
- Kim, M.; Cho, Y.; Park, S.; Huh, Y. *Cryst. Growth Des.* **2012**, *12*, 4180.
- Murray, B. J.; Li, Q.; Newberg, J. T.; Menke, E. J.; Hemminger, J. C.; Penner, R. M. *Nano Lett.* **2005**, *5*, 2319.
- Joo, T. H.; Kim, M. S.; Kim, K. *J. Raman Spectrosc.* **1987**, *18*, 57.
- Lee, J.; Lee, H.; Kim, K.; Shin, K. *Anal. Bioanal. Chem.* **2010**, *397*, 557.
- Nie, S.; Emory, S. R. *Science* **1997**, *275*, 1102.
- Upender, G.; Satyavathi, R.; Raju, B.; Shadak Alee, K.; Narayana Rao, D.; Bansal, C. *Chem. Phys. Lett.* **2011**, *511*, 309.
- Wan, L.; Terashima, M.; Noda, H.; Osawa, M. *J. Phys. Chem. B* **2000**, *104*, 3563.